

*Short Communication*

## **Effect of Antisite Defects on Li Ion Diffusion in LiNiPO<sub>4</sub>: a First Principles Study**

*Jianjian Shi*

Center for Public Security Information and Equipment Integration Technology, School of Physical Electronics, University of Electronic Science and Technology of China, Chengdu, 610054, P.R. China  
E-mail: [201511040203@std.uestc.edu.cn](mailto:201511040203@std.uestc.edu.cn)

*Received: 25 August 2016 / Accepted: 17 September 2016 / Published: 10 October 2016*

---

Lithium diffusion properties in crystalline LiNiPO<sub>4</sub> were studied using density functional theory. Formation and clustering energies of Li-Ni antisite defects are calculated, results showed the antisite defects are energetically favorable in the LiNiPO<sub>4</sub> and they not tend to bind together. The energy barrier of Li is 0.28 eV in the pristine LiNiPO<sub>4</sub>. The energy barriers of Li diffusion along the [010] direction in the LiNiPO<sub>4</sub> were not affected so much compared with that in the pristine system, however, the diffusion energy barrier of Ni diffusion was much larger than that of Li. This indicates that the existence of antisite defect will severely impede Li diffusion along the [010] direction and thus explains the poor cycling performance of LiNiPO<sub>4</sub> cathode materials for LIBs.

---

**Keywords:** Li ion batteries, DFT, antisite defects, cathode, LiNiPO<sub>4</sub>

### **1. INTRODUCTION**

The lithium ion batteries (LIBs) are considered as cheap energy storage devices, which exhibit promising applications in hybrid electric vehicles and all-electric vehicles [1, 2]. Developing of new cathode materials is very important for improving the charge capacity. Olivine-family lithium metal phosphate (LiMPO<sub>4</sub>, M=Fe, Mn, Ni, Co) cathode materials are the most promising ones due to their safety, environmental friendliness, low cost and high capacity [3-12]. Among the olive-type families, LiNiPO<sub>4</sub> is attracted more attention for its the highest voltage (about 5.1 V vs. Li/Li<sup>+</sup>). However, the obstacle for commercial application of LiNiPO<sub>4</sub> is its poor cycling performances, which are caused by its low intrinsic electronic and ionic conductivity. Several strategies have been used to improve the electrochemical performance of LiNiPO<sub>4</sub>, such as synthesizing LiNiPO<sub>4</sub>/C, graphitic carbon foams-LiNi<sub>1-y</sub>Mg<sub>y</sub>PO<sub>4</sub> composites and metal-doped LiNiPO<sub>4</sub> [11, 13-16]. The electrochemical properties of

$\text{LiNiPO}_4$  were improved via above methods, however the degradation mechanism of the pristine  $\text{LiNiPO}_4$  are not well understood. The electrochemical properties show great dependence on the structure stability of  $\text{LiNiPO}_4$ , therefore, it is essential to investigate the structure property and understand their chemistry to further enhance the cycling property of high voltage  $\text{LiNiPO}_4$  electrode materials for LIBs.

Olivine-type  $\text{LiNiPO}_4$  structure with space group of  $pnma$ , in which Li atoms occupy linear chains of edge-sharing octahedral along the  $[010]$  direction, whereas Ni atoms occupy zigzag chains of corner-sharing octahedral in the  $(011)$  plane. These chains are bridged by edge and corner shared phosphate tetrahedral, which create a rigid three-dimensional structure as shown in Fig. 1. The blue, green, red and grey balls represent the Ni, Li, O and P atoms, respectively. The  $\text{LiNiPO}_4$  has one-dimensional Li channels along the  $[010]$  direction. According to Devaraju et.al [12] observation using HAADF/ABF-STEM analysis show that antisite defects exists in  $\text{LiNiPO}_4$ , antisite defects means that Ni atoms occupy Li sites and Li occupy the Ni sites. The atomic scale investigations on the Li kinetic properties of  $\text{LiNiPO}_4$  with antisite defects are not understood.

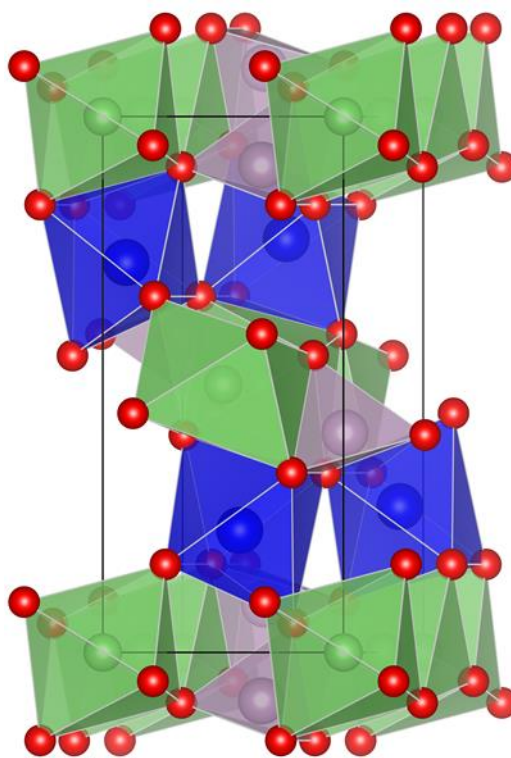


**Figure 1.** The crystallographic structure of  $\text{LiNiPO}_4$ . The blue, green, red and grey balls represent the Ni, Li, O and P atoms, respectively.

In this work, the formation and clustering energies of Li-Ni antisite defects, diffusion energy barriers for Li and Ni in the olivine-type  $\text{LiNiPO}_4$  system were studied using density functional theory (DFT). It is found that Li diffusion along the  $[010]$  direction is severely hindered by the antisite defect in  $\text{LiNiPO}_4$  and thus provides an insightful comprehension of the poor cycling performance of  $\text{LiNiPO}_4$  materials.

## 2. SIMULATION DETAILS

Li-Ni antisite defect formation energies, Li and Ni diffusion energy barriers were calculated using the SIESTA (Spanish Initiative for Electronic Simulations with Thousands of Atoms) code [17] based on DFT [18, 19]. The exchange-correlation energies were described using local density approximation (LDA) with the Ceperley-Alder (CA) functional [20, 21]. Numerical atomic orbits were described by using double zeta basis set plus polarization. A cutoff of 150 Ry was used for the Fourier expansion of the density. The unit cell of LiNiPO<sub>4</sub> was composed of 4Li, 4Ni, 4P and 16O atoms. A 3×7×7 k-point grid was used to optimize the atomic configuration by relaxing the atomic positions and cell parameters. Geometric optimization was done by conjugate gradients (CG) method until the force on every atom is smaller than 0.04 eV/Å. The calculated lattice constants for LiNiPO<sub>4</sub> are a=10.00 Å, b=5.75 Å, c=4.65 Å, which are great consistent with results of other groups [11, 12, 14, 15, 22, 23]. 1a×2b×3c LiNiPO<sub>4</sub> supercell was used to study the Li-Ni antisite defects.

The formation energies of Li-Ni antisite defects  $E_f(\text{Li} - \text{Ni})$  are calculated using the following equation [24, 25].

$$E_f(\text{Li} - \text{Ni}) = E_{\text{tot}}(\text{Li} - \text{Ni}) - E(\text{perfect}) \quad (1)$$

where  $E_{\text{tot}}(\text{Li} - \text{Ni})$  is the total energy of the LiNiPO<sub>4</sub> with Li-Ni antisite defects.  $E(\text{perfect})$  is total energy of the pristine bulk LiNiPO<sub>4</sub>.

The clustering energies  $E_{\text{clustering}}$  are calculated using the equation (2) [26].

$$E_{\text{clustering}} = E_f(\text{Li} - \text{Ni}) - nE_{\text{single-}f}(\text{Li} - \text{Ni}) \quad (2)$$

Here,  $E_{\text{single-}f}(\text{Li} - \text{Ni})$  is the formation energy of a single Li-Ni defect,  $n$  is the number of Li-Ni defects. A positive value of  $E_{\text{clustering}}$  indicates that Li-Ni antisite defects tend to separate each other when they are present in the samples.

## 3. RESULTS AND DISCUSSION

According to the symmetry of LiNiPO<sub>4</sub>, each Li atom has six neighboring Ni atoms with Li-Ni distance of 3.52, 3.60, and 3.08 Å, respectively. So Li-Ni<sub>1</sub>, Li-Ni<sub>2</sub> and Li-Ni<sub>3</sub> antisite defects may be formed, as shown in Fig. 2. The calculated formation energies of Li-Ni<sub>1</sub>, Li-Ni<sub>2</sub> and Li-Ni<sub>3</sub> antisite defects are 0.59, 0.54 and 0.57 eV, respectively. Low formation energies of defects generally mean that these defects form easily. The result indicates that these three kinds of Li-Ni antisite defects are energetically favorable in the LiNiPO<sub>4</sub>, which is consistent with the experimental observations [12]. This offers the theoretical evidence that the existence of Ni in Li positions and Li in Ni positions as antisite defects in the LiNiPO<sub>4</sub>.

In order to investigate how the antisite defect affects Li diffusion kinetics, the energy barriers of Li and Ni atoms diffusing from one octahedral to another octahedral site along the [010] diffusion channels were calculated. The calculated diffusion barrier of Li along the diffusion path in Fig. 3(b) in the pristine LiNiPO<sub>4</sub> is 0.28 eV, as shown in Fig.3 (a), which is in the range of reported values of 0.13~0.44 eV [27, 28]. The energy barriers of Li and Ni in the LiNiPO<sub>4</sub> with the existence of one pair

of Li-Ni antisite defect are 0.29 and 0.76 eV, respectively, as shown the green and blue curves in Fig. 4 (a). I-T-F and I'-T'-F' paths in Fig.4 (b) refer to Li and Ni diffusion pathways, respectively. Although the energy barrier value of Li in LiNiPO<sub>4</sub> with one Li-Ni is close to that of Li in the pristine LiNiPO<sub>4</sub>, however the value of diffusion barrier for Ni in Li sites along the [010] Li diffusion channels is 0.47 eV larger than that of Li. This suggests that Ni in Li sites will seriously hinder the diffusion of Li in the [010] Li diffusion channels.

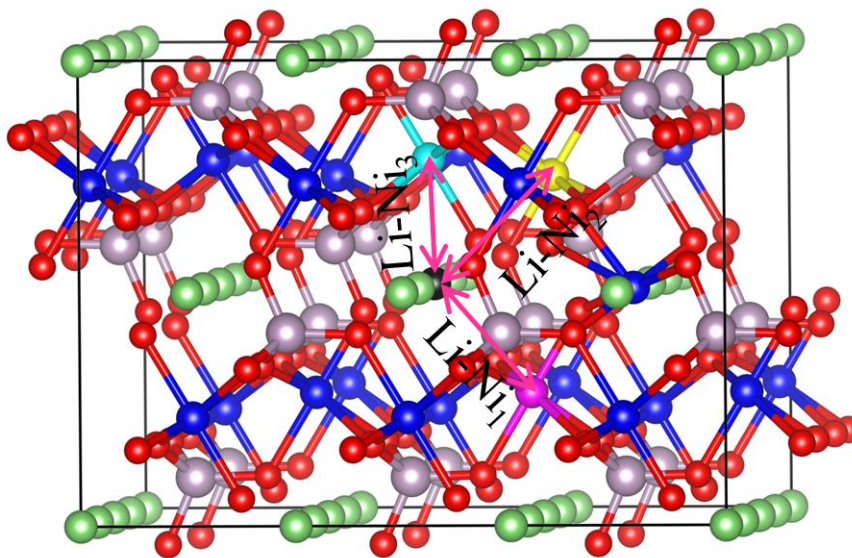


**Figure 2.** The crystallographic structure of the supercell LiNiPO<sub>4</sub>. The black ball represents one of Li atoms, it with the rosy (Ni<sub>1</sub>), yellow (Ni<sub>2</sub>) and sapphire (Ni<sub>3</sub>) balls consists of Li-Ni<sub>1</sub>, Li-Ni<sub>2</sub> and Li-Ni<sub>3</sub> three kinds of Li-Ni antisite defects, respectively.

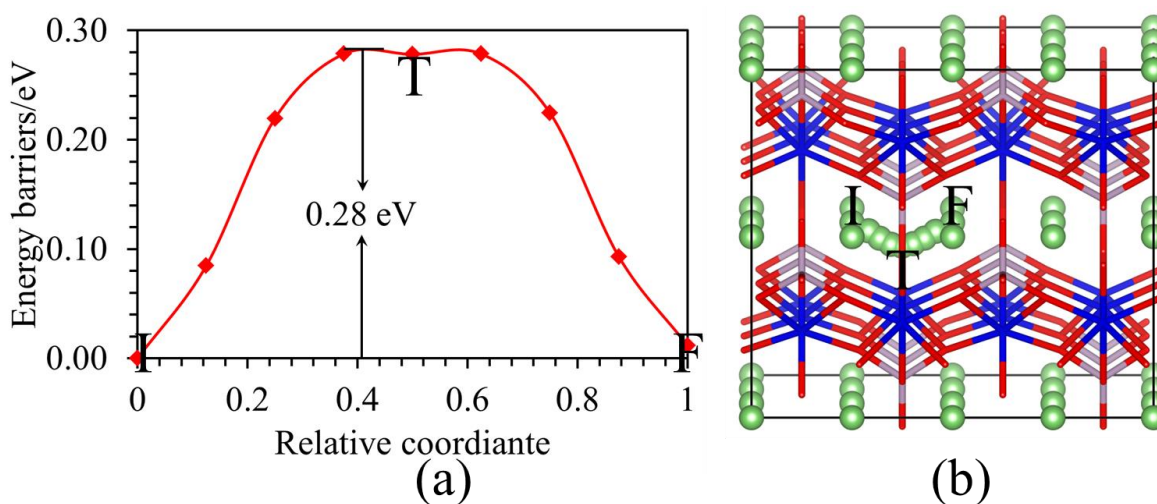


**Figure 3.** (a) The diffusion energy barrier curve for Li in the pure LiNiPO<sub>4</sub> supercell. (b) The diffusion pathway of Li along the [010] direction from one octahedral site to another adjacent octahedral site in the pure LiNiPO<sub>4</sub>.

Devaraju et al. reported that antisite defects are homogeneously distributed in  $\text{LiNiPO}_4$  [12]. Therefore, the clustering energy were calculated when more than one Li-Ni antisite defects exist. The calculated clustering energies are 0.11 and 0.12 eV for  $\text{LiNiPO}_4$  with two and three Li-Ni antisite defects, which demonstrate that the Li-Ni antisite defects do not tend to cluster. This is an agreement with the experiment observation that the antisite distributions are homogeneous [12]. Defects critically affect the properties of materials, thus, the defect concentration often plays a pivotal role in performance. Yildirim et al. [29] reported that the defect concentrations have an influence on the diffusion processes.

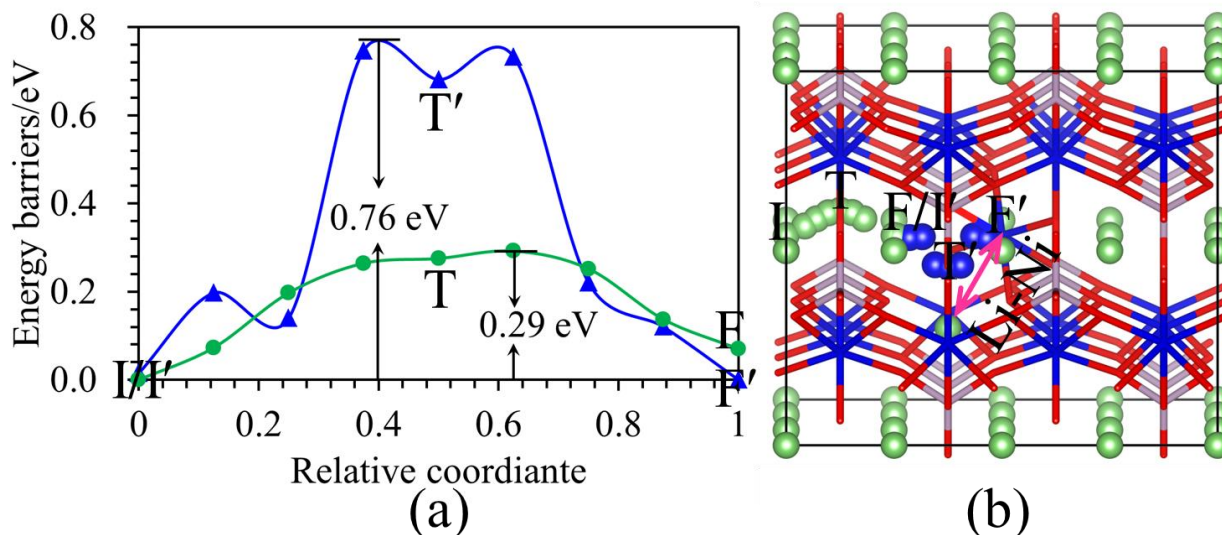
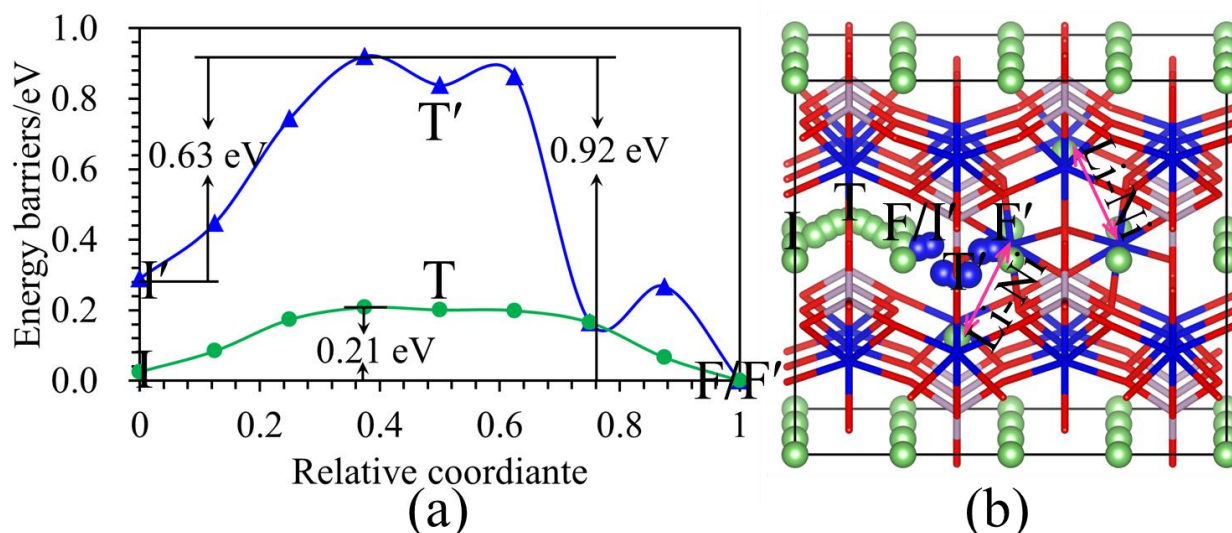


**Figure 4.** (a) The diffusion energy barrier curves for Li and Ni in the  $\text{LiNiPO}_4$  with one Li-Ni antisite defect. The green and blue curves correspond to Li and Ni energy barriers, respectively. (b) The diffusion pathways of Li and Ni in the  $\text{LiNiPO}_4$  with one antisite defect. I-T-F and I'-T'-F' paths correspond to Li and Ni, respectively.

Hence, it is necessary to further study the effect of the Li-Ni defects pairs on Li ion diffusion, the diffusion energy barriers of Li and Ni in the  $\text{LiNiPO}_4$  with two Li-Ni antisite defects were also calculated. The diffusion energy barrier is 0.21 eV for Li. However, the energy barrier for Ni along the I'-T'-F' path is 0.63 eV, along the F'-T'-I' path is 0.92 eV. The values of Ni in the  $\text{LiNiPO}_4$  with two pairs of antisite defects are less than 0.13 eV and more than 0.16 eV that that of Ni in the  $\text{LiNiPO}_4$  with one pair of defects along the I'-T'-F' and F'-T'-I' paths, respectively. The value of Li in the  $\text{LiNiPO}_4$  with two pairs of Li-Ni antisite defects is 0.07 smaller than in the pristine system. This suggests that the antisite defect concentrations have an influence on the Li and Ni diffusion. Although the diffusion barrier of Ni along the I'-T'-F' in two pairs of defects is smaller than in one pair, the values of Ni are still much larger than that of Li in the pure system. This resembles the results of the  $\text{LiNiPO}_4$  with one Li-Ni antisite defect that Ni also seriously hinder the diffusion of Li along the [010] diffusion channels in  $\text{LiNiPO}_4$  with two Li-Ni antisite defects.



J.J. Shi Figure 5

**Figure 5.** (a) The diffusion energy barrier curves for Li and Ni in the  $\text{LiNiPO}_4$  with two Li-Ni antisite defects. The green and blue curves correspond to Li and Ni energy barriers, respectively. (b) The diffusion pathways of Li and Ni in the  $\text{LiNiPO}_4$  with two antisite defects. I-T-F and I'-T'-F' paths correspond to Li and Ni, respectively.

On the basis of above discussions, Li-Ni antisite defects are energetically favorable in  $\text{LiNiPO}_4$  and not tend to cluster, which is consistent with the experimental results [12]. Moreover, antisite defects seriously hinder Li moving along the [010] direction in  $\text{LiNiPO}_4$ .

#### 4. CONCLUSIONS

Lithium ion diffusion in crystalline  $\text{LiNiPO}_4$  was studied using density functional theory. Formation and clustering energies show that Li-Ni antisite defects are energetically favorable in the  $\text{LiNiPO}_4$  and not tend to cluster. The result is great consistent with the experiment observation. The energy barriers of Ni in Li sites in the  $\text{LiNiPO}_4$  are great larger than those of Li in the  $\text{LiNiPO}_4$  system. This suggests that Ni in Li sites in  $\text{LiNiPO}_4$  system seriously hinder Li moving along the [010] diffusion channels and thus provides an insightful understanding of the poor cycling performance in  $\text{LiNiPO}_4$  system.

#### ACKNOWLEDGEMENT

This work was financially supported by the National Natural Science Foundation of China (11474047). This work was carried out at National Supercomputer Center in Tianjin, and the calculations were performed on TianHe-1(A).

#### References

1. S.M. Rommel, N. Schall, C. Brunig and R. Weihrich, *Monatsh Chem* 145 (2014) 385.

2. Y. Lin, Y. Yang, R. Yu, H. Lai and Z. Huang, *Journal of Power Sources* 259 (2014) 188.
3. Y. Zhang, H.J. Zhang, Y.Y. Feng, L. Fang and Y. Wang, *Small* 12 (2016) 516.
4. T.-F. Yi, Z.-K. Fang, Y. Xie, Y.-R. Zhu and C. Dai, *Journal of Alloys and Compounds* 617 (2014) 716.
5. R. Trócoli, S. Franger, M. Cruz, J. Morales and J. Santos-Peña, *Electrochimica Acta* 135 (2014) 558.
6. L.F.J. Piper, N.F. Quackenbush, S. Sallis, D.O. Scanlon, G.W. Watson, K.W. Nam, X.Q. Yang, K.E. Smith, F. Omenya, N.A. Chernova and M.S. Whittingham, *The Journal of Physical Chemistry C* 117 (2013) 10383.
7. J. Yang and J.S. Tse, *J Phys Chem A* 115 (2011) 13045.
8. F.C. Strobridge, D.S. Middlemiss, A.J. Pell, M. Leskes, R.J. Clément, F. Pourpoint, Z. Lu, J.V. Hanna, G. Pintacuda, L. Emsley, A. Samoson and C.P. Grey, *J Mater Chem A* 2 (2014) 11948.
9. M.K. Devaraju, Q.D. Truong, T. Tomai, H. Hyodo, Y. Sasaki and I. Honma, *RSC Adv.* 4 (2014) 52410.
10. J.L. Allen, T. Thompson, J. Sakamoto, C.R. Becker, T.R. Jow and J. Wolfenstine, *Journal of Power Sources* 254 (2014) 204.
11. Y. Zhang, Y. Pan, J. Liu, G. Wang and D. Cao, *Chem Res Chinese U* 31 (2015) 117.
12. M.K. Devaraju, Q.D. Truong, H. Hyodo, Y. Sasaki and I. Honma, *Sci Rep* 5 (2015) 11041.
13. M. Prabu, S. Selvasekarapandian, A.R. Kulkarni, S. Karthikeyan and C. Sanjeeviraja, *Transactions of Nonferrous Metals Society of China* 22 (2012) 342.
14. M. Mumtaz, N.K. Janjua, A. Yaqub and S. Sabahat, *Journal of Sol-Gel Science and Technology* 72 (2014) 56.
15. R. Qing, M.-C. Yang, Y.S. Meng and W. Sigmund, *Electrochimica Acta* 108 (2013) 827.
16. L. Dimesso, C. Spanheimer and W. Jaegermann, *Mater Res Bull* 48 (2013) 559.
17. J.M. Soler, E. Artacho, J.D. Gale, A. Garcia, J. Junquera, P. Ordejon and D. Sanchez-Portal, *J Phys-Condens Mat* 14 (2002) 2745.
18. F. Legrain, O. Malyi and S. Manzhos, *Journal of Power Sources* 278 (2015) 197.
19. F. Legrain, O.I. Malyi and S. Manzhos, *Comp Mater Sci* 94 (2014) 214.
20. L.J. Sham, *Philos T Roy Soc A* 334 (1991) 481.
21. D.M. Ceperley and B.J. Alder, *Phys Rev Lett* 45 (1980) 566.
22. R. Cheruku, G. Kruthika, G. Govindaraj and L. Vijayan, *J Phys Chem Solids* 86 (2015) 27.
23. S. Karthickprabhu, G. Hirankumar, A. Maheswaran, R.S. Daries Bella and C. Sanjeeviraja, *Ionics* 21 (2014) 345.
24. H. Duan, J. Li, H. Du, S.W. Chiang, C. Xu, W. Duan and F. Kang, *The Journal of Physical Chemistry C* 119 (2015) 5238.
25. K. Hoang and M. Johannes, *Chemistry of Materials* 23 (2011) 3003.
26. H. Guo, X. Song, Z. Zhuo, J. Hu, T. Liu, Y. Duan, J. Zheng, Z. Chen, W. Yang, K. Amine and F. Pan, *Nano letters* DOI 10.1021/acs.nanolett.5b04302(2015).
27. D. Morgan, A. Van der Ven and G. Ceder, *Electrochemical and Solid-State Letters* 7 (2004) A30.
28. C.A.J. Fisher, V.M.H. Prieto and M.S. Islam, *Chemistry of Materials* 20 (2008) 5907.
29. H. Yildirim, A. Kinaci, M.K.Y. Chan and J.P. Greeley, *ACS applied materials & interfaces* 7 (2015) 18985.